In Vivo Long-Term Kinetics of Radiolabeled *N*,*N*-Dimethyltryptamine and Tryptamine

Arturo A. Vitale[1], Alicia B. Pomilio[1], Carlos O. Cañellas[2], Martín G. Vitale[1], Eva Maria Putz[1,3], and Jorge Ciprian-Ollivier[4]

[1]*PRALIB (CONICET, UBA), Facultad de Farmacia y Bioquímica, Universidad de Buenos Aires, Buenos Aires, Argentina;* [2]*Tecnonuclear S.A., Buenos Aires, Argentina;* [3]*University of Vienna, Vienna, Austria; and* [4]*Centro de Psiquiatría Biológica de Buenos Aires, Universidad de Buenos Aires, Buenos Aires, Argentina*

N,*N*-dimethyltryptamine (DMT), a strong psychodysleptic drug, has been found in higher plants, shamanic hallucinogenic beverages, and the urine of schizophrenic patients. The aim of this work was to gain better knowledge on the relationship between this drug and hallucinogenic processes by studying DMT behavior in comparison with tryptamine. **Methods:** ^{131}I-labeled DMT and tryptamine were injected into rabbits. γ-Camera and biodistribution studies were performed. Brain uptake, plasma clearance, and renal excretion were assessed for each indolealkylamine. **Results:** DMT and tryptamine showed different behavior when brain uptake, residence time, and excretion were compared. Labeled DMT entered the brain 10 s after injection, crossed the blood–brain barrier, and bound to receptors; then it was partially renally excreted. It was detected in urine within 24 h after injection and remained in the brain, even after urine excretion ceased; up to 0.1% of the injected dose was detected at 7 d after injection in the olfactory bulb. In contrast, tryptamine was rapidly taken up in the brain and fully excreted 10 min after injection. **Conclusion:** To our knowledge, this is the first demonstration that exogenous DMT remains in the brain for at least 7 d after injection. Although labeled DMT and tryptamine behave as agonists for at least 5-hydroxytryptamine 2A receptor, 5-hydroxytryptamine 2C receptor, trace amine-associated receptor, and σ-1 putative receptor targets, binding to the latter can explain the different behavior of labeled DMT and tryptamine in the brain. The persistence in the brain can be further explained on the basis that DMT and other *N*,*N*-dialkyltryptamines are transporter substrates for both the plasma membrane serotonin transporter and the vesicle monoamine transporter 2. Furthermore, storage in vesicles prevents DMT degradation by monoamine oxidase. At high concentrations, DMT is taken up by the serotonin transporter and further stored in vesicles by the vesicle monoamine transporter 2, to be released under appropriate stimuli. Moreover, the ^{131}I-labeling proved to be a useful tool to perform long-term in vivo studies.

Key Words: ^{131}I-*N*,*N*-dimethyltryptamine; ^{131}I-tryptamine; planar imaging studies

J Nucl Med 2011; 52:970–977
DOI: 10.2967/jnumed.110.083246

In continuation of our research on labeled compounds, such as phenethylamines, tryptamines, and harmines and native Amazonian *N*,*N*-dimethyltryptamine (DMT)–containing beverages such as ayahuasca (*1–3*) (also called ayahoasca and hoasca tea), we now report the in vivo behavior of DMT and tryptamine.

DMT (Fig. 1) is a psychodysleptic compound that has been found in a variety of higher plants (*4,5*) and organisms (*6*), brain and other tissues of mammals and humans (*6,7*), and the urine of schizophrenic patients (*2,8–10*).

As a hallucinogen, DMT was reported as a direct postsynaptic agonist at 5-hydroxytryptamine 2A (5-HT_{2A}) receptors and a partial agonist at 5-hydroxytryptamine 2C (5-HT_{2C}) receptors (*11*). Recently, biochemical, physiologic, and behavioral experiments demonstrated that DMT is an endogenous agonist at σ-1 receptors (σ-1Rs) (*12*); the hypothetical signaling scheme triggered by this binding has also been reported (*13*). These facts, together with our intention to provide insight into this issue, led us to develop in vivo DMT (compared with tryptamine) studies in animal models.

Therefore, DMT and tryptamine were labeled with ^{131}I and administered to rabbits to follow the uptake, residence time, and clearance in the brain. Labeling with ^{131}I was suitable because of its long half-life (8.05 d) and the possibility of assessing clearance from brain by planar imaging for several days.

Iodine is covalently bonded to these indolealkylamines, and by this methodology we have a direct insight of what is going on in vivo. Previous reports on radiolabeled 2-iodoindolealkylamines, such as serotonin (*14*) and melatonin (*15*), demonstrated that iodinated and noniodinated indole compounds had a similar behavior with respect to ligand–receptor interactions (*16*). Nevertheless, for both

Received Sep. 11, 2010; revision accepted Feb. 18, 2011.
For correspondence or reprints contact: Arturo A. Vitale, Research Institute, PRALIB (CONICET, UBA), Facultad de Farmacia y Bioquímica, Universidad de Buenos Aires, Junín 956, C1113AAD Buenos Aires, Argentina.
E-mail: avitale@ffyb.uba.ar or aavitale@sinectis.com.ar

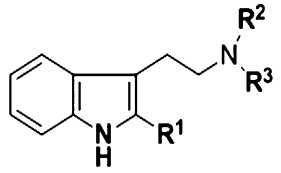

Compound	R^1	R^2	R^3
N,*N*-dimethyltryptamine (DMT)	H	CH_3	CH_3
Tryptamine (T)	H	H	H
2-iodo-*N*,*N*-dimethyltryptamine (2-I-DMT)	I	CH_3	CH_3
2-iodo-tryptamine (2-I-T)	I	H	H

FIGURE 1. Chemical structures of DMT, tryptamine, 2-I-DMT, and 2-I-T.

2-iodo-*N*,*N*-dimethyltryptamine (2-I-DMT) and 2-iodo-tryptamine (2-I-T) we can consider that there are at least 3 putative receptor targets, for example, 5-HT receptors, σ-1Rs, and trace amine-associated receptors (TAARs).

MATERIALS AND METHODS

Tryptamine was purchased from Aldrich, and carrier-free $Na^{131}I$ was supplied by Comisión Nacional de Energía Atómica. DMT was prepared in the laboratory. Solvents were purified to high purity before use and checked by gas chromatography (GC). Thin-layer chromatography (TLC) was performed on silica gel 60 F_{254} and alumina plates (Merck); spots were visualized under ultraviolet light (254 nm) and in an iodine chamber. Direct electron impact mass spectra (EI-MS) and gas chromatography MS (GC-MS) analyses were achieved on a Trio2 VG spectrometer at 70 eV with helium as carrier. A fused silica SPB-1 capillary column (Sigma-Aldrich; 30 m length × 0.20 mm internal diameter [ID]) was used. In addition, the following program temperature was used: 60°C for 1 min, 60°C–290°C (10°C/min), and 5 min at 290°C, and mass scanning range, 30–500. Melting points (MPs) were recorded in a Fisher-Johns apparatus and were uncorrected. ^{1}H- (200 MHz) and ^{13}C- (50.3 MHz) nuclear magnetic resonance (NMR) spectra were recorded in a Bruker ACE 200 in $CDCl_3$. Infrared spectra were recorded in a Mattson 3000 FT-IR spectrometer.

Labeled samples were counted in an automatic γ-detector (Clinigamma Pharmacia). A Sigma 400 γ-camera (Ohio Nuclear) was used for planar imaging.

Preparation of DMT

DMT was prepared as reported previously (*17*). *Indole-3-methyl acetate* was prepared in a 95% yield by esterification of indole-3-acetic acid: a solution of indole-3-acetic acid (1 g; 5.3 mmol) in methanol (70 mL), with a few drops of sulfuric acid as catalyst, was heated under reflux for 2 h until the indoleacetic acid had completely disappeared, as checked by TLC on alumina plates using ethyl acetate as a solvent (acid R_f, 0.1; ester R_f, 0.9). The solution was neutralized with $CaCO_3$ and filtered, and the solvent was evaporated under reduced pressure. The product was crystallized from methanol to give 0.95 g (5.0 mmol; 95%) of indole-3-methyl acetate (MP, 48.0°C–48.5°C). The carbonyl of the ester was assessed by infrared (1,722 cm^{-1} C=O).

N,N-Dimethyltryptamide. Indole-3-methyl acetate was dissolved in 40% aqueous solution (20 mL) of dimethylamine and further stirred at 20°C for 40 h. The reaction was monitored by TLC (silica gel–ethyl acetate) (amide R_f, 0.5; ester R_f, 0.8). The excess of dimethylamine was evaporated at 20°C under reduced pressure to avoid hydrolysis. The product was filtered and purified by sublimation to give 0.8 g of *N*,*N*-dimethyltryptamide (4 mmol; 80%; MP, 119°C–120°C). The carbonyl of the amide was assessed by infrared (1,630 cm^{-1} C=O).

DMT. N,N-dimethyltryptamide (0.4 g, 1.98 mmol), dissolved in dry dichloromethane (25 mL), was added slowly to a stirred suspension of $LiAlH_4$ (0.4 g, 10.5 mmol) in dry tetrahydrofuran (15 mL). The mixture was stirred for 48 h at 25°C under nitrogen until the amide had completely disappeared—checked by TLC (silica gel–methanol) (amine R_f, 0.2; amide R_f, 0.8). The excess of $LiAlH_4$ was decomposed with water and ice. The reaction mixture was filtered under vacuum and dried over anhydrous $MgSO_4$, and solvents were removed. The yield was 76% (0.28 g, 1.5 mmol) of a colorless oil, which crystallized in the freezer (−20°C) after a week (MP, 44°C–45°C; fumarate MP, 152°C–153°C).

Spectra of DMT (17). **^{1}H-NMR** (δ): 2.39 (6H, s; N-C**H**$_3$); 2.68 (2H, t; H-β); 2.95 (2H, t; H-α); 6.98 (1H, s; H-2); 7.11 (1H, dt; J_o 8.5 Hz; J_m 1.9 Hz; H-6); 7.15 (1H, dt; J_o 8.5 Hz; J_m 1.9 Hz; H-5); 7.35 (1H, dd; J_o 8.5 Hz; J_m 1.9 Hz; H-7); 7.65 (1H, dd; J_o 8.5 Hz; J_m 1.9 Hz; H-4); 8.14 (1H, bs; indole N**H**). **^{13}C-NMR** (δ_C): 23.7 (s, C-β); 45.5 (p, N-**C**H$_3$); 60.4 (s, C-α); 107.6 (t, C-7); 111.2 (q, C-3); 118.8 (t, C-5); 119.1 (t, C-4); 121.5 (t, C-6); 121.9 (t, C-2); 127.2 (q, C-4a); 136.1 (q, C-7a). p: primary carbon; s: secondary carbon; t: tertiary carbon; q: quaternary carbon. **EI-MS *m/z* (%):** 188 ($M^{+\cdot}$; 13); 143 (M-45; 28); 130 (M-58; 100); 77 (M-130; 20); 58 ($H_2C{=}N^+Me_2$; 90); 42 (40). **GC retention time (tR):** 10.10 min. **High-Resolution–Mass Spectrometry (HR-MS):** $C_{12}H_{16}N$ calculated, 188.131349; found, $M^{+\cdot}$ 188.131295.

Iodination of DMT (17). DMT (0.10 g; 0.53 mmol) in chloroform (5 mL) was added to a solution of chloramine-T (0.15 g, 0.73 mmol) in water (5 mL). An aqueous solution of potassium iodide (0.12 g, 0.73 mmol) was added to the reaction mixture, further stirred for 15 min, and decolored with sodium metabisulfite (0.02 g, 0.10 mmol). The organic layer was dried with anhydrous $MgSO_4$, and the solvent was removed under reduced pressure to obtain a light yellow oil (0.14 g, 0.45 mmol) of 2-I-DMT (yield, 85%).

Spectra of 2-I-DMT: ***^{1}H-NMR.*** (δ) 2.29 (6H, s; N-C**H**$_3$); 2.35 (2H, t; H-β); 2.62 (2H, t; H-α); 7.15 (1H, dt; J_o 8.5 Hz; J_m 1.9 Hz; H-6); 7.33 (1H, dt; J_o 8.5 Hz; J_m 1.9 Hz; H-5); 6.95 (1H, dd; J_o 8.5 Hz; J_m 1.9 Hz; H-7); 7.45 (1H, dd; J_o 8.5 Hz; J_m 1.9 Hz; H-4); 8.18 (1H, bs; indole N**H**). **^{13}C-NMR**: (δ_C) 20.8 (s, C-β); 45.3 (p, N-**C**H$_3$); 59.1 (s, C-α); 84.2 (q, C-2); 111.7 (t, C-7); 118.4 (t, C-4); 119.1 (t, C-5); 121.5 (q, C-3); 125.5 (t, C-6); 129.1 (q, C-4a); 141.7 (q, C-7a). **EI-MS *m/z* (%):** 314 ($M^{+\cdot}$, 5); 300 (8); 186 (M-128; 100); 171 (M-143; 40); 130 (M-184; 60); 71 (15). **GC t_R:** 9.98 min. **HR-MS:** $C_{12}H_{15}IN_2$ calculated, 314.027955; found, $M^{+\cdot}$ 314.028001. Tryptamine was iodinated in a manner similar to DMT iodination. Experimental details have been previously reported (*17*). Spectra (^{1}H-, ^{13}C-NMR, and EI-MS) of 2-I-T agreed with those previously reported (*17*). The purity of each compound was checked by GC and was higher than 99%.

Spectra of 2-I-T: ***^{1}H-NMR.*** (δ) 1.24 (2H, bs; N**H**); 2.84 (2H, t; H-β); 2.98 (2H, t; H-α); 7.07 (1H, dt; J_o 8.5 Hz; J_m 1.9 Hz; H-6); 7.12 (1H, dt; J_o 8.5 Hz; J_m 1.9 Hz; H-5); 7.29 (1H, dd; J_o 8.5 Hz; J_m 1.9 Hz; H-7); 7.53 (1H, dd; J_o 8.5 Hz; J_m 1.9 Hz; H-4); 8.15 (1H, bs;

indole NH). **^{13}C-NMR** (δ_C) 23.8 (s, C-β); 48.9 (s, C-α); 87.1 (q, C-2); 109.3 (t, C-7); 111.5 (t, C-4); 117.9 (t, C-5); 118.5 (q, C-3); 121.1 (t, C-6); 126.2 (q, C-4a); 138.2 (q, C-7a). **EI-MS *m/z* (%):** 286 ($M^{+\cdot}$, 12); 256 (M-30; 52); 158 (M-128; 12); 30 (M-256; 100). **GC t_R:** 9.77 min. **HR-MS:** $C_{11}H_{13}N_2$ calculated, 286.019945; found, $M^{+\cdot}$, 286.0184093.

Labeling Step: Radioiodination of DMT and Tryptamine. The organic compound, DMT or tryptamine (1 mg), was dissolved in dichloromethane (0.5 mL). Two layers were formed when Na[^{131}I] (111 MBq) in a sodium hydroxide aqueous solution was added. An aqueous solution of chloramine-T (1 mL of 1.5 mg/mL) was added dropwise to this mixture under stirring. The reaction occurred in 15 min. The free iodine was reduced with 0.5 mL of a sodium thiosulfate solution (0.05 g of sodium thiosulfate in a 1-mL solution of HCl/water), thus being extracted into the aqueous layer. Both organic and aqueous layers (OL and AL, respectively) were separately γ-counted. The chloroform layer (OL) was evaporated to dryness, and the iodinated amine was dissolved in 200 μL of phosphate-buffered saline (pH 7.4). The reaction was tested by TLC (alumina/benzene:acetone, 7:10, v/v) (^{131}I-2-I-DMT R_f, 0.10; ^{131}I R_f, 0.45). Blank assays were performed. ^{131}I-2-I-DMT was retained in the OL. The counting of both layers (OL and AL) led to a coefficient of 0.10 ± 0.05 using r = OL/(AL + OL). TLC analysis of the OL supported the experimental radioiodination parameters.

^{131}I-2-I-DMT. Labeling efficiency (%) equaled ([OL − AL] × r)/(OL + AL) × 100 = 81.6; radiochemical purity (RP %) equaled ([OL − AL] × r)/OL × 100 = 98.0; and RP % by TLC was 98.5.

^{131}I-2-I-T. Labeling efficiency (%) equaled ([OL − AL] × r)/(OL + AL) × 100 = 90.0; radiochemical purity (RP %) equaled ([OL − AL] × r)/OL × 100 = 99.0; and RP % by TLC was 99.0.

Both ^{131}I-labeled indolealkylamines, ^{131}I-2-I-DMT and ^{131}I-2-I-T, were obtained with high labeling efficiency and high radiochemical purity.

Lipophilicity of Molecules. The lipophilicity of the molecules was assessed by the separate determination of both *n*-octanol/water partition coefficients of ^{131}I-2-I-DMT and ^{131}I-2-I-T.

Neutrality of Molecules. The ionic charge was determined by electrophoresis in Whatman No. 1 paper at 300 V for 60 min with 5 mM buffer phosphate solutions at pH 6.5, 6.8, 7.3, and 7.5, under conditions similar to those of the plasmatic and cerebral compartments.

In Vivo Studies

All animal experiments were performed according to the rules of the Bioethical Committee of CONICET and Universidad de Buenos Aires and in accordance with the internationally accepted principles in the care and use of experimental animals. In vivo studies were performed with inbred male rabbits (weight, ~2,500 g [10 ± 2 g of brain weight]). Rabbits (n = 9) were housed in individual metabolic cages, fed standard rabbit chow, and allowed water ad libitum. A 12-h light period was used. Rabbits were catheterized in the marginal ear vein, by which normal saline and each ^{131}I-indolealkylamine dose was injected. The activity of each administered radiolabeled compound was 11.1 MBq of ^{131}I-indolealkylamine/kg of rabbit body weight.

Planar Imaging

Animals were placed in the γ-camera in the ventral decubitus position on the detector crystal. Images (128 × 128) were acquired every 10 s until 3 min, then every 30 s until 60 min, and afterward (64 × 64) at 90, 120, 180, 240, and 360 min and 7 d after injection. Regions of interest were the brain, heart, kidneys, liver, and bladder. Plots of clearance and decays were obtained for the target organs.

Plasma Clearance

Blood samples were collected at different times in vials of known weight and then measured in an automatic γ-detector. The results were expressed as counts per minute (cpm) per gram of blood; specific activity (SA) was determined after decay correction. Data were plotted as *ln* SA versus time, with a linear correlation greater than 0.9. Both short and long half-lives ($t_{1/2}$) were calculated.

Renal Excretion

Twenty-four-hour urine samples were collected after injection. Urine aliquots were chromatographed in Whatman No. 1 paper/chloroform:acetic acid (9:1) (^{131}I-2-I-DMT R_f, 0.9; radioactive and iodine) and in TLC (silica gel/MeOH) (^{131}I-2-I-DMT R_f, 0.4; radioactive and iodine). Spots were visualized in an iodine atmosphere and further measured in the γ-detector. Spots of the excreted labeled compounds were compared with those of the injected labeled indolealkylamine. Furthermore, a sterile urine sample was obtained 5 min after injection by catheterization. Urine was immediately worked up under inert conditions (N_2) to avoid oxidative artifacts. It was alkalinized with 10% sodium hydroxide and extracted with dichloromethane. Radioactivity was checked in both ALs and OLs to verify in which layer were the labeled DMT metabolites. After 10-fold concentration, the positive radioactive layer was analyzed by GC-MS.

Distinct Brain Structure Uptake

Inbred rabbits (n = 3) in which the brain uptake had been previously evaluated in a γ-camera were used. Rabbit brain (n = 3) was extirpated at 48 h after injection and kept cold. Olfactory bulb (OB), olfactory peduncle (OP), olfactory tubercle (OT), cerebral cortex (CC), cerebellum, and medulla oblongata (MO) were separated out. Each portion was homogenized and taken to volume with normal saline. Radioactivity of each homogenate was measured in the γ-detector. To test whether this activity was due to labeled DMT, a 10% sodium hydroxide solution was added and then extracted with dichloromethane. The organic layer was dried over anhydrous sodium sulfate, and an aliquot was chromatographed using TLC in the same way as reported for urine. ^{131}I-2-I-DMT was used as a standard. Radioactivity of the aqueous layer was also checked.

Statistical Analysis

Standard ANOVA and the Student *t* test were used. A *P* value of 0.05 or less was applied as the statistical significance criterion.

RESULTS

Preparation of DMT

DMT was freshly prepared with 99.5% purity in our laboratories, releasing the free base from the fumarate derivative just before use. DMT was protected from light and oxygen for experiments.

Radioiodination of DMT and Tryptamine

DMT and tryptamine (Fig. 1) were radioiodinated in good yields and high radiochemical purity (≥98%), with an SA of 100 MBq/mg. Radiolabeled DMT and tryptamine were lipophilic and neutral molecules as shown by *n*-octanol/water partition coefficients and electrophoresis at various pH values, respectively.

Planar Imaging

Labeled DMT and tryptamine were injected into the rabbit ear vein. The dose was 0.10 mg/kg, equivalent to that of 0.06–0.40 mg/kg injected in human studies (*18*). The kinetics of labeled DMT was studied in vivo by planar imaging; the regions of interest were the brain, liver, and heart.

Serial images from 10 to 200 s of DMT uptake in the heart, brain, kidneys, and bladder are shown in Figure 2. The immediate entry into the brain compartment is clearly observed. Side effects due to drug administration were not detected.

After labeled DMT distribution in organs, activity in the liver and heart decreased, whereas activity in the brain remained constant. The only organs that recorded an increase of activity were the kidneys because of the rapid renal clearance of DMT from the animal body into the urine. Time–activity plots were obtained for the brain, heart, and liver (Fig. 3).

According to the kinetics of brain uptake (Fig. 3A), at 10 s after injection 87.5% of the maximum dose was taken up by the brain, which reached the maximum at 30 s after injection. At 5 min after injection, 20.0% ± 2.2% (5 μg/g of brain) of the ID was in the brain (Fig. 4), decreasing to 2.1 ± 0.5 %ID at 60 min, when the excretion was 70.1 ± 5.5 %ID.

Static images at 60 min (Fig. 5A) and 90 min after injection (Fig. 5B) showed that the activity remained in the brain and concentrated in the OB (Fig. 5C) after 240 min.

Plasma Clearance

During a 60-min γ-camera recording, activity was detected only in plasma up to 10–12 min. The analysis of SA as a function of time for labeled DMT led to short and long $t_{1/2}$. The first $t_{1/2}$, 5.0 ± 0.8 min (short), accounted for brain uptake, and the second, 29.0 ± 3.1 min (long) for renal excretion. Results were decay-corrected. The kinetics of plasma clearance was almost asymptotic, as shown in Figure 3B. After 10 s after injection, 45 %ID had been cleared from this compartment, decreasing slowly until more than 90 min. No myocardial uptake was observed after 240 min. The kinetics of hepatic uptake (Fig. 3C) showed a slower clearance than plasma, exhibiting a slight slope.

Renal Excretion

Renal excretion of labeled DMT at different times is shown in Table 1.

A urine sample obtained by catheterization 5 min after injection was analyzed by GC-MS to identify the excreted metabolites. After alkalinization and extraction with dichloromethane, radioactivity was checked in both the AL and the OL. Radioactivity was found only in the OL. Therefore, we continued analyzing the OL by GC-MS to identify the compounds. MS accounted for 2-I-DMT. Further chromatography of this aliquot (TLC and Whatman No. 1 systems) showed the same R_f as that of the radiolabeled pure compound. The radioactivity and R_f of the spot of labeled DMT were coincident with those of the spot stained with iodine.

Distinct Brain Structure Uptake

To establish DMT static distribution in the brain, the activities of the OB, OP, OT, CC, cerebellum, and MO were measured as shown in Figure 6. Seven days after injection, 0.1 %ID (0.025 μg/g of brain) was still detected in brain. To test whether the radioactivity of the OB homogenate was due to DMT, a 10% sodium hydroxide solution was added and further extracted with dichloromethane. An aliquot of the organic layer obtained after work-up was chromatographed on TLC in the same manner as reported for urine.

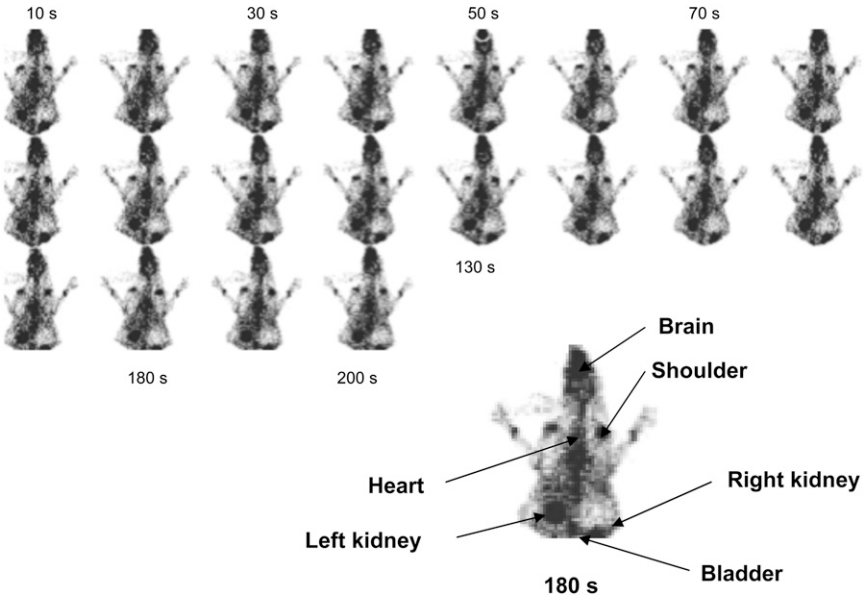

FIGURE 2. Planar images of distribution of labeled DMT after administration via ear vein. Images (128 × 128) were obtained from γ-camera every 10 s (image 1) until 200 s (image 20).

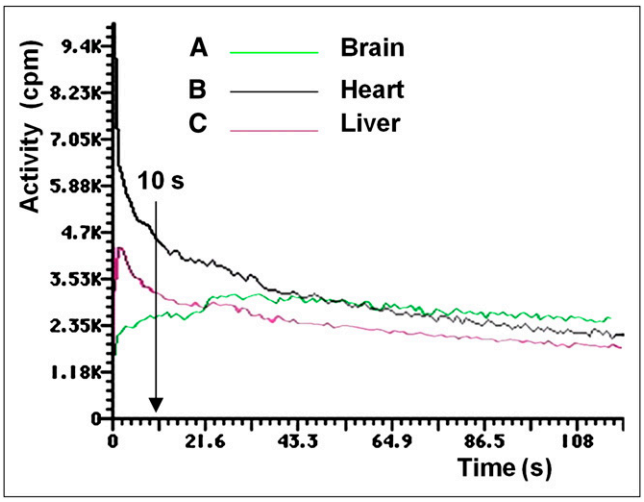

FIGURE 3. Activity vs. time plots of brain, heart, and liver uptake of labeled DMT. In the brain at 10 s after injection, 87.5% of maximum dose was taken up, reaching maximum at 30 s after injection. At 10 s after injection, 45 %ID had been cleared from heart to the plasma. Hepatic uptake showed slower clearance than plasma, exhibiting a slight slope.

Both spots of the ^{131}I-2-I-DMT standard and of the sample showed the same R_f. No other radioactive compound was detected. To determine whether there were any other metabolites, the AL was measured in the γ-counter, and no activity was detected.

Tryptamine

By contrast, tryptamine entered the brain and was completely excreted in the urine 20 min after injection. The comparative activity of DMT and tryptamine in the brain over time is shown in Figure 7.

DISCUSSION

The aim of this work was to study the in vivo comparative behavior of both labeled DMT and tryptamine in the brain. The γ-emitter ^{131}I was selected for labeling to perform long-term studies because it decays with a half-life of 8.05 d.

Each lipophilic and neutral labeled indolealkylamine (DMT and tryptamine) was injected into rabbits, went directly through the bloodstream to the brain, and crossed the blood–brain barrier, according to planar imaging.

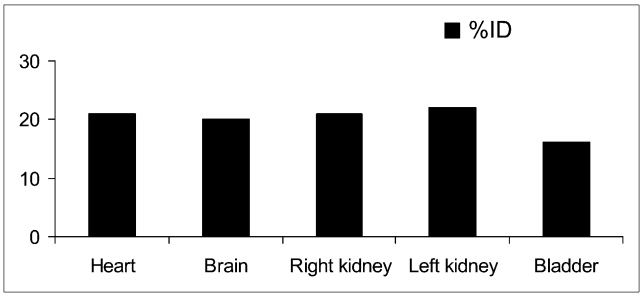

FIGURE 4. Biodistribution of labeled DMT in rabbits at 5 min after injection.

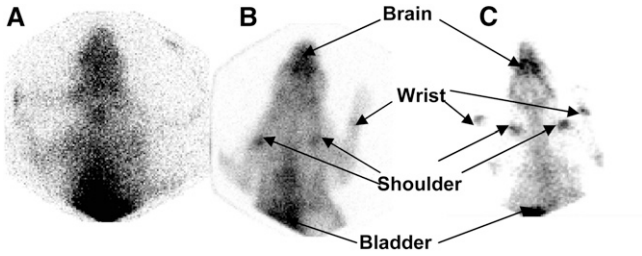

FIGURE 5. Biodistribution of labeled DMT in rabbits: at 60 min after injection (A), 90 min after injection (B), and 240 min after injection (C) of labeled DMT (29.6 MBq).

Both compounds showed remarkably different behavior when being compared for brain uptake, residence time, and excretion. Rapid brain uptake and clear urine excretion were observed for tryptamine, which was fully excreted at 10 min after injection (Fig. 7). In contrast, DMT entered the brain 10 s after intravenous injection, crossed the blood–brain barrier, and was only partially renally excreted. Moreover, DMT remained in the brain after 48 h and was still detected at 7 d after injection. There were no traces of either DMT or any other labeled compound in the urine at 24 h after injection. Therefore, DMT was unable to be released from the brain beyond a certain point, and even after being completely cleared from the blood, DMT was still present in the brain. Part of the injected DMT could not be removed from the synaptosome.

Chromatographic analysis showed that DMT was excreted unchanged in urine—analysis supported by the EI-MS. DMT administered intravenously behaves differently from orally administered DMT, which would be subjected to oxidative deamination by digestive monoamine oxidase (MAO-A) and subsequent enzymatic degradation by aldehyde-dehydrogenase into indoleacetic acid. The administration route plays an important role (*18*).

The detection of unmetabolized DMT in urine agrees with our previous results on the identification of intact DMT in the urine of schizophrenics and ayahoasca drinkers (*1,2*). One plausible explanation is that exogenous labeled DMT intravenously administered goes to the heart, where it is pumped out through arterial circulation to the organs,

TABLE 1
Renal Excretion of Labeled DMT at Different Times

Time	%ID
10 min	8.0 ± 1.3
20 min	34.5 ± 4.7
30 min	50.1 ± 3.9
60 min	70.1 ± 5.5
24 h	80.0 ± 8.5

Data are mean ± SD.

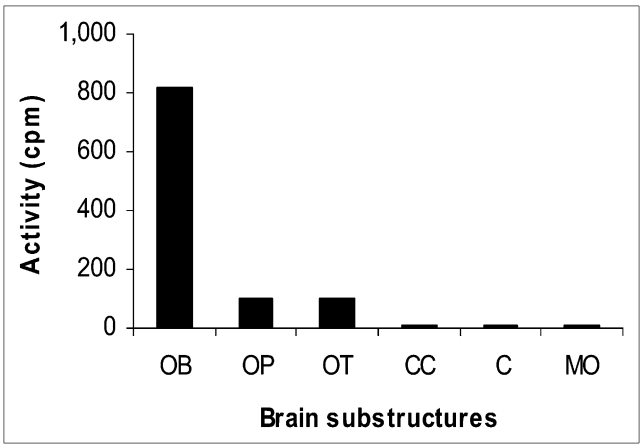

FIGURE 6. Activity of each rabbit brain substructure after labeled DMT administration: OB, 816 ± 51 cpm; OP, 101 ± 12 cpm; OT, 96 ± 9 cpm; CC, 5 ± 2 cpm; cerebellum, 5 ± 2 cpm; and MO, 5 ± 2 cpm. C = cerebellum.

mainly the brain and kidneys (where it is excreted into urine). Intracellular MAOs, for example, platelet and leukocyte MAO (MAO-B), and the soluble extracellular plasma semicarbazide-sensitive amine oxidase, or serum amine oxidase, occur in blood. From all these enzymes, solely extracellular circulating MAO enzymes, for example, serum amine oxidase, would be able to metabolize labeled DMT. However, the rabbit serum amine oxidase deaminates only primary amines (*19*). Secondary and tertiary amines, as well as α-substituted amines, are not attacked. Therefore, DMT is not a substrate of this MAO.

When DMT and tryptamine are compared, the only structural difference is the presence of the *N,N*-dimethylamino group and primary amino group, respectively, giving rise to a distinguished interaction with receptors. According to reported evidence (*11*), DMT is a direct postsynaptic agonist at the 5-HT_{2A} receptor and a partial agonist at the 5-HT_{2C} receptor. The latter, but not 5-HT_{2A}, shows a deep desensitization to DMT over time. This direct 5-HT agonism decreases the rate of serotonin synthesis and turnover in the brain (*20*)—a result that has been proposed as the basis of the psychodysleptic effects of DMT (*21*). During hallucinations, dynamic connectivity alterations matched with increased activity in specific cortical regions (*22*). Cortical 5-HT_{2A} receptors were also found on presynaptic, putatively dopaminergic, monoaminergic axons and synapses, on astrocytes, and on γ-aminobutyric acid-ergic interneurones (*21*).

According to our results, the labeled DMT that remained in the brain at 48 h after injection was concentrated in the OB, followed by OP and OT (Fig. 6). The olfactory system is important in the life of a rabbit, for feeding and social contacts (*23*). The OB is one of the major forebrain targets of the ascending serotonin pathway (*24*) and is located at the start of a hierarchic chain of sensory processing mechanisms (*23,25*). Olfactory receptors in mammals transduce their signals to intracellular cyclic adenosine monophosphate (cAMP) signaling (*26*). The development of odor memory to conditioned odor training is associated with the phosphorylation of cAMP response element binding protein in the OB (*27*). This type of odor conditioning has also been linked to 5-HT receptors, β-adrenoceptors, and extrinsic noradrenergic modulation (*23*). β-adrenergic stimulation increases cAMP in mitral cells, an effect that requires 5-HT–induced mobilization of Ca^{2+}.

The 5-HT_{1A} autoreceptors play a key role in regulating brain emotional responses associated with the amygdala (*28*), which is involved in the mammal social functions. There is a significant inverse relationship between the density of the 5-HT_{1A} autoreceptors and the amygdala reactivity to threatening stimuli, thus reflecting the effects of 5-HT_{1A} on the negative feedback loop that controls serotonin release (*25*).

Some DMT behavior did not involve the 5-HT or other monoaminergic systems (*29*), and the DMT-enhanced phosphatidylinositol production was not blocked by the 5-HT_{2A} receptor antagonist ketanserin (*30*). Therefore, 5-HT receptors are not the sole mediators of DMT psychodysleptic effects.

DMT is in small concentrations an agonist at the TAARs, thus activating adenylcyclase and resulting in cAMP accumulation (*31*). TAARs, together with at least 2 other receptor families, for example, odorant and vomeronasal-type receptors, are involved in the detection of volatile chemical stimuli (*32*). The involvement of TAARs is further supported by the fact that DMT is a potent elicitor of cAMP accumulation as tryptamine or LSD (*33*). However, it is unclear whether TAARs are associated with psychodysleptic effect, and controversies have arisen concerning TAARs involved in schizophrenic symptomatology (*13*). There is

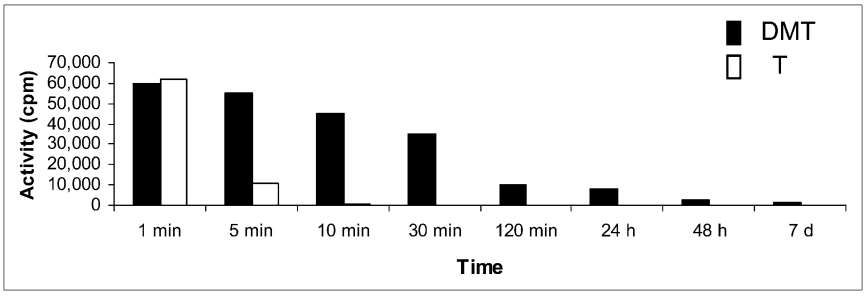

FIGURE 7. Comparative activity of DMT and tryptamine (T) in rabbit OB and OP over time.

no difference between DMT and tryptamine in this regard to account for the observed differential behavior.

DMT also binds to σ-1Rs at low micromolar concentrations, inhibits voltage-activated sodium ion channels via σ-1R interactions at higher concentrations, and induces hypermobility in wild-type mice (*12*). An important biologic activity of σR activation is the inhibition of ion channels through protein–protein interactions without mediation by G proteins and protein kinases (*34,35*). The σ-1R pharmacophore includes an alkylamine core. Therefore, *N,N*-dimethylated compounds, such as DMT, bind σ-1Rs tightly (dissociation constant [K_D] = 14.75 μM) and are much stronger than tryptamine (K_D = 431.55 μM). Furthermore, DMT modulates σ-1 chaperone activity and affects ion channels at micromolar concentrations (*12*).

According to our results, labeled DMT remains in the brain for much longer than labeled tryptamine. Because both labeled indolealkylamines behave as agonists for at least 3 putative receptor targets, for example, 5-HT (mainly 5-HT_{2A} and 5-HT_{2C}), TAARs, and σ-1, the fact that in vivo binding of DMT is stronger than that of tryptamine can be somehow explained by the latter receptors, supported by the reported K_D values measured in vitro (*12*). However, the persistence in the brain requires further analysis.

Active uptake processes may concentrate DMT by severalfold, resulting in micromolar concentrations in the brain. A mechanism to reach high local DMT concentrations within neurons is probably via a 2-step process involving uptake across the plasma membrane, followed by sequestration into synaptic vesicles. The interaction of several hallucinogenic tryptamines with plasma membrane monoamine uptake transporters has been previously reported (*36*). Cozzi et al. (*37*) demonstrated that DMT and related compounds are transporter substrates, not uptake blockers, for both the plasma membrane serotonin transporter and the neuronal vesicle monoamine transporter 2 and that there are separate substrate and inhibitor binding sites within these transporters. DMT interacts with both transporters with more affinity than serotonin (*37*). Therefore, DMT is transported into the cytosol or into vesicles by serotonin transporter or vesicle monoamine transporter 2, respectively (*37*).

At high concentrations, DMT is taken up by serotonin transporter and further stored in vesicles by vesicle monoamine transporter 2 to be released under appropriate stimuli. Once inside a neuron, DMT can reach intracellular binding sites and be stored within synaptic vesicles for subsequent release as a transmitter substance; DMT can also be released from vesicles into the cleft to interact with cell surface σ-1Rs, 5-HT receptors, or other molecular targets.

This combination of mechanisms may explain our findings about the long-term DMT persistence in the brain, together with the fact that storage in vesicles prevents DMT degradation by MAO.

In summary, this work offers an in vivo model of what might be happening in the brain with high doses of exogenous DMT.

CONCLUSION

Visual hallucinations seem to be associated with complex dynamic alterations of brain connectivity, which have wide clinical significance. This work contributes to a deeper understanding of the behavior of DMT in vivo. After injecting labeled DMT, physiologic and biochemical effects occurred because of the action on mainly 3 putative receptor targets: 5-HT_2 (5-HT_{2A} and 5-HT_{2c}) receptors, TAARs, and σ-1Rs.

Our findings in vivo agree with the in vitro study findings of Fontanilla et al. (*12*) and Cozzi et al. (*37*). As a substrate for transporters, DMT can be accumulated in vesicles to reach relatively high levels and to function as a releasable transmitter.

To our knowledge, this is the first report on the demonstration that exogenous DMT, having completed urine excretion 24 h after injection, remains in the brain at least 7 d after injection. Furthermore, the ^{131}I labeling proved to be a useful tool for long-term in vivo studies.

DISCLOSURE STATEMENT

The costs of publication of this article were defrayed in part by the payment of page charges. Therefore, and solely to indicate this fact, this article is hereby marked "advertisement" in accordance with 18 USC section 1734.

ACKNOWLEDGMENTS

AAV and ABP are Research Members of CONICET, Argentina.

This study was supported in part by the University of Buenos Aires (Argentina) and the National Research Council of Argentina (CONICET) and training fellowships from IAESTE International (London, U.K.) and MINCYT (Relaciones Internacionales, Argentina) (EMP).

REFERENCES

1. Pomilio AB, Vitale AA, Ciprian Ollivier J, Cetkovich Bakmas M, Gómez R, Vázquez G. Ayahoasca: an experimental psychosis that mirrors the transmethylation hypothesis of schizophrenia. *J Ethnopharmacol.* 1999;65:29–51.
2. Pomilio AB, Vitale A, Ciprian Ollivier J, Cetkovich Bakmas MA. Chemical approach to the understanding of schizophrenia. *An Asoc Quim Argent.* 1998;86:320–335.
3. Pomilio AB, Vitale A, Ciprian Ollivier J. Cult-*Hoasca*: a model for schizophrenia. *Mol Med Chem.* 2003;1:1–7.
4. Buchanan MS, Carroll AR, Pass D, Quinn RJ. NMR spectral assignments of a new chlorotryptamine alkaloid and its analogues from *Acacia confusa. Magn Reson Chem.* 2007;45:359–361.
5. Tempone AG, Sartorelli P, Teixeira D, et al. Brazilian flora extracts as source of novel antileishmanial and antifungal compounds. *Mem Inst Oswaldo Cruz.* 2008;103:443–449.
6. Jacob MS, Presti DE. Endogenous psychoactive tryptamines reconsidered: an anxiolytic role for dimethyltryptamine. *Med Hypotheses.* 2005;64:930–937.
7. Barker SA, Monti JA, Christian ST. *N,N*-dimethyltryptamine: an endogenous hallucinogen. *Int Rev Neurobiol.* 1981;22:83–110.
8. Checkley SA, Murray RM, Oon MC, Rodnight R, Birley JL. A longitudinal study of urinary excretion of *N,N*-dimethyltryptamine in psychotic patients. *Br J Psychiatry.* 1980;137:236–239.

9. Ciprian-Ollivier J, Cetkovich-Bakmas MG. Altered consciousness states and endogenous psychoses: a common molecular pathway? *Schizophr Res.* 1997; 28:257–265.
10. Phillips ML. Understanding the neurobiology of emotion perception: implications for psychiatry. *Br J Psychiatry.* 2003;182:190–192.
11. Smith RL, Canton H, Barrett RJ, Sanders-Bush E. Agonist properties of *N,N*-dimethyltryptamine at serotonin 5-HT_{2A} and 5-HT_{2C} receptors. *Pharmacol Biochem Behav.* 1998;61:323–330.
12. Fontanilla D, Johannessen M, Hajipour AR, Cozzi NV, Jackson MB, Ruoho AE. The hallucinogen *N,N*-dimethyltryptamine (DMT) is an endogenous σ-1 receptor regulator. *Science.* 2009;323:934–937.
13. Su T-P, Hayashi T, Vaupel DB. When the endogenous hallucinogenic trace amine *N,N*-dimethyltryptamine meets the σ-1 receptor. *Sci Signal.* 2009;2:pe12.
14. Attanasio A, Rager K, Gupta D. Ontogeny of circadian rhythmicity for melatonin, serotonin, and *N*-acetylserotonin. *J Pineal Res.* 1986;3:251–256.
15. Niles LP, Pickering DS, Sayer BG. HPLC-purified 2-[^{125}I]iodomelatonin labels multiple binding sites in hamster brain. *Biochem Biophys Res Commun.* 1987;147:949–956.
16. Cohen H, Mertens J, Maziere B. *Radioiodination reaction for radiopharmaceuticals. Compendium of effective strategies synthesis.* Dordrecht, The Netherlands: Springer; 2006.
17. Sintas JA, Vitale AA. Synthesis of ^{131}I derivatives of indolealkylamines for brain mapping. *J Labelled Comp Radiopharm.* 1997;39:677–684.
18. Strassman R. *DMT: The Spirit Molecule: A Doctor's Revolutionary Research into the Biology of Near-Death and Mystical Experiences.* Rochester, VT: Park Street Press, a Division of Inner Traditions International; 2001.
19. McEwen CM Jr., Sober AJ. Rabbit serum monoamine oxidase. II. Determinants of substrate specificity. *J Biol Chem.* 1967;242:3068–3078.
20. Stahl SM. *Stahl's Essential Psychopharmacology: Neuroscientific Basis and Practical Applications*. 3rd ed. Cambridge, NY: Cambridge University Press; 2008.
21. Kalat JW. *Biological Psychology.* 10th ed. Belmont, CA: Wadsworth Pub Co.; 2009.
22. Ffytche DH. The hodology of hallucinations. *Cortex.* 2008;44:1067–1083.
23. O'Connor S, Jacob TJC. Neuropharmacology of the olfactory bulb. *Curr Mol Pharmacol.* 2008;1:181–190.
24. Dahlström A, Fuxe K. Evidence for the existence of monoamine neurons in the central nervous system. II. Experimentally induced changes in the intraneuronal amine levels of bulbospinal neurons systems. *Acta Physiol Scand Suppl.* 1965; (suppl 247):1–36.
25. Descarries L, Riad M, Parent M. Ultrastructure of the serotonin innervation in the mammalian central nervous system. In: Müller CP, Jacobs BL, eds. *Handbook of Behavioral Neuroscience.* Burlington, VT: Elsevier BV, Academic Press; 2010:65–101.
26. Krautwurst D. Human olfactory receptor families and their odorants. *Chem Biodivers.* 2008;5:842–852.
27. McLean JH, Harley CW, Darby-King A, Yuan Q. pCREB in the neonate rat olfactory bulb is selectively and transiently increased by odor preference-conditioned training. *Learn Mem.* 1999;6:608–618.
28. Fisher PM, Meltzer CC, Ziolko SK, Price JC, Hariri AR. Capacity for $5HT_{1A}$ mediated autoregulation predicts amygdala reactivity. *Nat Neurosci.* 2006;9: 1362–1363.
29. Jenner P, Marsden CD, Thanki CM. Behavioural changes induced by *N,N*-dimethyltryptamine in rodents. *Br J Pharmacol.* 1980;69:69–80.
30. Deliganis AV, Pierce PA, Peroutka SJ. Differential interactions of dimethyltryptamine (DMT) with 5-HT_{1A} and 5-HT_2 receptors. *Biochem Pharmacol.* 1991;41:1739–1744.
31. Borowsky B, Adham N, Jones KA, et al. Trace amines: identification of a family of mammalian G protein-coupled receptors. *Proc Natl Acad Sci USA.* 2001; 98:8966–8971.
32. Ray LB. Biogenic amine receptors. *Sci Signal.* 2009;2:ec231.
33. Bunzow JR, Sonders MS, Arttamangkul S, et al. Amphetamine, 3,4-methylenedioxymethamphetamine, lysergic acid diethylamide, and metabolites of the catecholamine neurotransmitters are agonists of a rat trace amine receptor. *Mol Pharmacol.* 2001;60:1181–1188.
34. Aydar E, Palmer CP, Klyachko VA, Jackson MB. The σ receptor as a ligand-regulated auxiliary potassium channel subunit. *Neuron.* 2002;34:399–410.
35. Johannessen M, Ramachandran S, Riemer L, Ramos-Serrano A, Ruoho AE, Jackson MB. Voltage-gated sodium channel modulation by *sigma*-receptors in cardiac myocytes and heterologous systems. *Am J Physiol Cell Physiol.* 2009; 296:C1049–C1057.
36. Nagai F, Nonaka R, Kamimura KSH. The effects of non-medically used psychoactive drugs on monoamine neurotransmission in rat brain. *Eur J Pharmacol.* 2007;559:132–137.
37. Cozzi NV, Gopalakrishnan A, Anderson LL, et al. Dimethyltryptamine and other hallucinogenic tryptamines exhibit substrate behavior at the serotonin uptake transporter and the vesicle monoamine transporter. *J Neural Transm.* 2009; 116:1591–1599.